Sampling Polymorphs of Ionic Solids using Random Superlattices

Vladan Stevanović[1,2,*]

[1]*Colorado School of Mines, Golden, Colorado 80401, USA*
[2]*National Renewable Energy Laboratory, Golden, Colorado 80401, USA*

Polymorphism offers rich and virtually unexplored space for discovering novel functional materials. To harness this potential approaches capable of both exploring the space of polymorphs and assessing their *realizability* are needed. One such approach devised for partially ionic solids is presented. The structure prediction part is carried out by performing local density functional theory relaxations on a large set of random supperlattices (RSLs) with atoms distributed randomly over different planes in a way that favors cation-anion coordination. Applying the RSL sampling on MgO, ZnO, and SnO_2 reveals that the resulting probability of occurrence of a given structure offers a measure of its realizability explaining fully the experimentally observed, metastable polymorphs in these three systems.

The discovery of polymorphism in the late 18th and early 19th century [1,2] revealed the significance of structural degrees of freedom in determining physical properties of solids. The best known example is probably elemental carbon with markedly different mechanical, optical, and electronic properties between its graphite and diamond forms [3]. Other notable cases include white and gray tin, which also exhibit significant differences in electronic and mechanical properties [3], or enhanced photocatalytic activity of anatase TiO_2 compared to the ground state rutile polymorph [4], or elemental silicon, an indirect band-gap semiconductor in the ground state diamond structure predicted to become a direct gap material in a number of higher energy structures [5] including the experimentally realized clathrate structure [6].

However, the development of rational approaches to explore the space of polymorphs and (desirably) assist in their experimental realization faces significant challenges. First, the complexity of the potential energy surface (PES) of periodic systems, evidenced by the exponential increase in the number of local minima with the system size [7], limits our ability to systematically explore the spectrum of possible structures.

A related problem of finding the ground state structure attracted attention, especially with the development of first-principles total energy methods, resulting in a number of structure prediction techniques [8,9]. These include simulated annealing [10,11], methods based on evolutionary algorithms [12–15], metadynamics [16,17], basin and minima hopping [18,19], random structure searching [20], methods based on data mining and machine learning [21], structure prototyping [22–24], etc. Although focused on finding the ground state structure, some of these methods were also used in exploring the space of polymorphs (see, for example, Refs. [5,24–26]) with the energy above the ground state

as the main quantifier of their potential for experimental realization.

This brings us to the second major challenge, the assessment of the likelihood for experimental realization of different polymorphs. While certainly being an important quantity, the energy above the ground state alone is insufficient to explain observations based on available experimental data. For example, in the case of MgO, despite predictions [25], only the ground state rocksalt structure, and no other, is experimentally realized as reported in the Inorganic Crystal Structure Database [27]. In the case of ZnO, only the ground state wurtzite and two other structures, zinc blende and rocksalt, are experimentally realized [27–29]. Another important example is SnO_2, which undergoes a series of phase transitions under pressure [30], but all of the high pressure phases relax to either the ground state rutile or the metastable α-PbO_2 structure type upon releasing the pressure [31]. These facts indicate that for a given composition there seems to exist a finite set of structures that have higher likelihood for realization than the rest.

If this is true, then the realizability of a given polymorph can be thought of as determined by a combination of three factors: (i) the energy above the ground state, (ii) the energy barrier to escape from a given PES minimum, and (iii) the volume of configuration space occupied by the PES minimum. (i) and (ii) describe the principles of energy minimization and kinetic trapping. The factor (iii), on the other hand, measures the probability of getting into a given PES minimum. More precisely, as shown in Fig. 1, every local minimum on the PES defines its basin of attraction, or the region of configuration space that has that minimum as its "center of gravity." Hence, the probability of "falling" into a certain structure has to be proportional to the total volume of configuration space occupied by its basin of attraction including all of the symmetry equivalent basins.
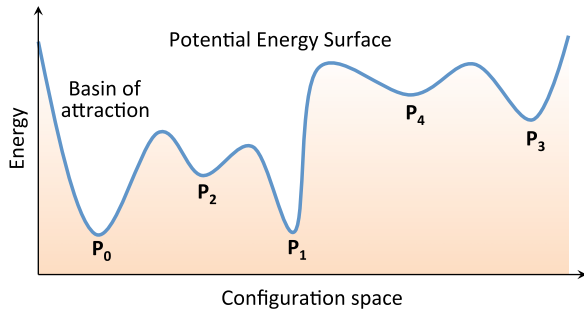
FIG. 1.   A sketch of the potential energy surface of solids with different polymorphs corresponding to different PES local minima.

FIG. 2.   Steps in the random superlattice structure generation (see text for details).

Similar arguments were presented recently by De *et al.* [32] in the context of the experimental realizability of finite size systems (i.e., clusters).

Motivated by the general features of the potential energy surfaces of solids that are discussed in more detail in Ref. [20] (and the references therein) it is demonstrated here, using MgO, ZnO, and SnO_2 as case examples, that factor (iii) is actually critical in establishing a ranking of realizability with (i) and (ii) providing additional constraints. This is done by pursuing the idea that the total volume occupied by various basins of attraction can be estimated using a large number of random structures (random unit cell vectors and random atomic positions) that are relaxed to the closest PES local minimum utilizing density functional theory (DFT). The frequency of occurrence of a given structure would then provide an estimate of the probability to fall into its local minimum.

To do this, and, at the same time, to overcome in part the difficulties posed by the already mentioned complexity of the PES together with the fact that the volume of attraction basins is ill defined in truly infinitely periodic systems, the size of the simulation cell is constrained and a structure prediction method is proposed to bias the random sampling toward the region of the PES more relevant for ionic systems. Because of the charge transfer only the structures that have cations preferentially coordinated by anions and vice versa are relevant. The method adopted here favors the cation-anion coordination by distributing different types of ions in a random fashion over two interpenetrating grids of points. The grids are constructed using the alternating planes of a superlattice defined by a randomly chosen reciprocal lattice vector (see Fig. 2). Constructed in this way, these random superlattice (RSL) structures exhibit dominant cation-anion coordination.

For each MgO, ZnO, and SnO_2 a total of 2000 RSL structures with sizes varying between 1 and 20 f.u. are constructed and DFT relaxed to the closest local minimum. The relaxed structures are sorted into classes of equivalence and for the classes with largest occupancies (frequencies of occurrence) additional phonon calculations are performed with the purpose of providing the information on the dynamic stability. The analysis of the resulting frequencies of occurrence shown in Figs. 3 and 4 reveals that the experimentally observed polymorphs are exclusively the ones with the highest occurrence.
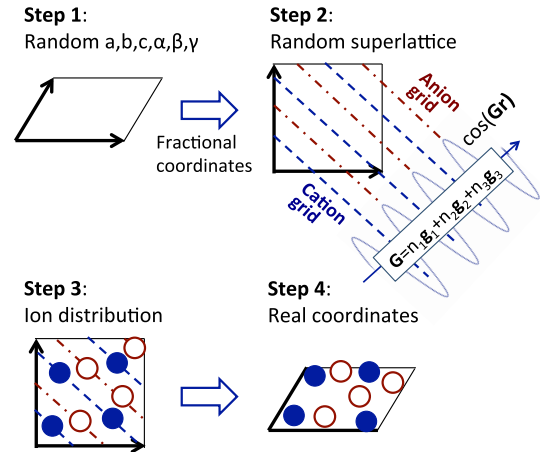
RSL sampling.—The details of the RSL structures' generation are shown in Fig. 2. It is a modification of the *ab initio* random structure searching method [20] and similarly starts with the random choice of unit cell parameters a, b, c, α, β, γ. In the second step the cation and anion grids are constructed in the following way. First, a transformation to the fractional (crystal) coordinates is performed to provide a cubiclike representation of the unit cell. Then, a reciprocal lattice vector $\mathbf{G} = n_1\mathbf{g}_1 + n_2\mathbf{g}_2 + n_3\mathbf{g}_3$ with random n_1, n_2, n_3 is constructed. $\mathbf{G}$ defines a plane wave $\cos(\mathbf{G}\mathbf{r})$ and an associated superlattice. The two grids are constructed by discretizing the planes corresponding to the minima (cation grid) and the maxima (anion grid) of the plane wave. In the third step the ions are distributed over the two grids. To ensure homogeneous distribution and that no two ions of the same kind are too close, the probability distribution is constructed by placing a Gaussian centered at each occupied grid point. The next ion is then placed on a grid point chosen randomly among those that have low probability. Finally, the structure is converted from fractional back into the real coordinates and the scaling factor is adjusted such that the minimal distance between any two atoms is larger than a certain threshold. The example of an RSL structure of ZnO shown in the Supplemental Material [33] clearly displays the dominant cation-anion coordination.

A total of 6000 RSL structures are generated (2000 per system) with the following parameters: a, b, and c randomly chosen between 0.6 and 1.4 (in units of *scale*); α, β, and γ random in the (30°,160°) range; n_1, n_2, and n_3 also random between 4 and 10, the range which ensures a sufficient, but not too large, number of planes in the unit cell; and the *scale* is adjusted such that the shortest distance
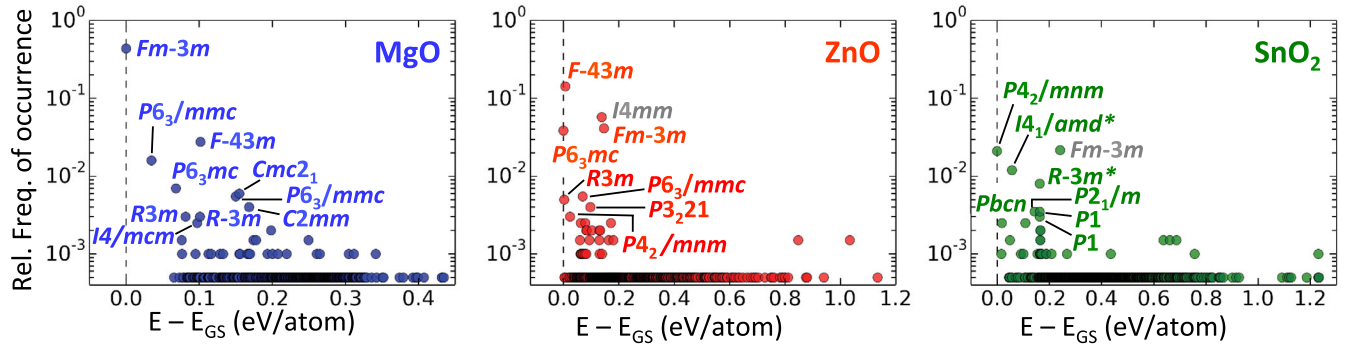
FIG. 3.   Relative frequencies of the occurrence of structures resulting from the RSL sampling shown against the energy above the ground state. Only the top occurring structures have their space groups explicitly marked. Space groups shown in gray represent the structures that are predicted to be dynamically unstable. The $I4_1/amd$ (anatase) and R-$3m$ SnO_2 structures are marked with asterisks as they appear only for small cell sizes (see text for discussion).

between the atoms is not shorter than 1.8 Å. Different unit cell sizes are sampled by creating the RSL structures with 1–20 f.u. and 100 RSLs per size. The allternative would be to fix the cell size, but this would bias the sampling only to structures with sizes compatible with the chosen one. Another important reason for sampling over different cell sizes is that some PES minima may appear large in low dimensions, but are actually small when the number of dimensions increases. These will likely not have high chances for experimental realization because the nucleation and growth of bulk phases typically start at the nanometer scale. The ranges of cell sizes within which structures appear (provided in Tables I, II, and III in the Supplemental Material [33]) are important indicators of this effect.

DFT calculations.—Full relaxations, including volume, cell shape, and atomic positions, are performed on all RSL structures. This is done by employing the standard DFT approach [34] with the PBE form of the exchange-correlation functional [35] and the projector augmented wave (PAW) method [36] as implemented in the VASP code [37]. The employed numerical setup (**k**-points, various cutoffs) results in absolute total energies that are converged to within 3 meV/atom. All relaxations (volume, shape, atomic positions) are conducted using the conjugate gradient algorithm [38]. For numerical reasons, the relaxation procedure (both volume and ions) has been restarted at least 4 times followed by a self-consistent run. For all structures with total final pressure exceeding 3 kbar and/or forces exceeding 10^{-4} eV/Å additional restarts have been performed until these criteria are achieved. Construction of the work flows, management of the large number of calculations, and analysis of results is carried out using the *pylada* software [39].

Structure sorting.—Sorting of the resulting, DFT-relaxed, structures into the classes of equivalence is done based on four criteria. Two structures are considered equivalent if (1) their total energies are within 10 meV/atom, (2) their space groups match, (3) their volumes per atom are within 0.5%, and (4) the coordination of atoms up to the 4th

neighbor is the same. Because of very low symmetry of the starting RSL structures as well as numerical inaccuracies that remain after DFT relaxation, the tolerances for both the space group and coordination shells determination were set to a relatively generous 0.1 Å. Increasing the tolerance factors to 0.3 Å does not affect final results. After extensive testing these criteria were proven robust in establishing equivalence between the structures.

Note that because of the size and coordination constraints imposed in the sampling procedure as well as some dependence of the final structure on the relaxation algorithm, the population of each class is an estimate, rather than an accurate measure, of the basin volume. Furthermore, because DFT relaxations could potentially drive the system across very small local minima and assign parts of configuration space to larger nearby basins, the sampling procedure adopted here actually estimates the volume of configuration space that "funnels" toward a given larger minimum. To indicate this difference, the term *funnel* of attraction will be used from here on instead of the term *basin* of attraction.

Results.—The RSL sampling procedure combined with DFT relaxations results in 904 distinct structure types (classes of equivalence) for MgO, 1306 for ZnO, and 1740 for SnO_2. Figure 2 in the Supplemental Material [33] shows for all three systems the number of distinct structures within various energy windows above the ground state as a function of the total number of structures used in sampling. Two observations can be made. First, there are clear differences between the PESs of MgO, ZnO, and SnO_2, evidenced by a different number of distinct structures present in the corresponding windows. Second, for all three systems the number of distinct structures grows monotonically with little or no sign of convergence. This implies that even within a relatively narrow energy range a very large number of structures can potentially be found, including low energy structures with defects and/or interfaces between low energy structures.

Fortunately, however, a vast majority of structures that result from the RSL sampling are actually irrelevant for their very low probability (frequency) of occurrence. As shown in Fig. 3, except for a relatively small number of structures that occur more frequently, nearly all other polymorphs occur only once. Moreover, if the frequency of occurrence is represented as a function of the total number of structures the extrapolation to the infinite number of structures would imply zero probabilities for all of these. In contrast, all of the top occurring structures have their frequencies of occurrence fairly converged with the total number of structures used in sampling.

In the case of MgO, the top occurring is the rocksalt Fm-$3m$ structure with the relative frequency of occurrence of 0.437 far above any other structure. It is followed by the zinc blende F-$43m$, and a four atom $P6_3/mmc$ structure with the relative frequencies of 0.0275 and 0.016, respectively. The occurrence of all other structures is below 0.01. It is not a surprise then that the rocksalt is the only experimentally realized MgO phase. Furthermore, for all cell sizes the rocksalt MgO is consistently the top occurring structure (Table I in the Supplemental Material [33]).

The RSL sampling of ZnO polymorphs results in the distribution of the relative frequencies such that four distinct structures occur more frequently than the others. These are the ground state wurtzite $P6_3mc$, zinc blende F-$43m$, tetragonal $I4mm$, and the rocksalt Fm-$3m$. Phonon calculations reveal that the tetragonal $I4mm$ shown in gray in Fig. 3 is dynamically unstable. The remaining three are exactly the three known, experimentally realized polymorphs of ZnO [27–29]. Furthermore, all three polymorphs consistently appear as the top occurring structures for all cell sizes.

The ZnO results support directly the previous discussion about the energy above the ground state and its inadequacy to judge the realizability of different polymorphs. Namely, as shown in Fig. 3, there is a large number of distinct structures that appear inside the ~150 meV/atom energy window between the ground state wurtzite and the rocksalt structure. A significant fraction of these have their volumes smaller than wurtzite. It is, however, the rocksalt that is realized by applying the pressure despite its relatively high energy. Based on these results it can be argued that the realization of the rocksalt phase is due to its relatively large funnel of attractions. Of course, for the polymorph to be metastable the kinetic barriers need to be sufficiently high to provide the conditions for the kinetic trapping, which is an experimental fact for both zinc blende and rocksalt ZnO [27–29]. However, it is the volume of configuration space that comes first in determining the list of candidate structures with higher likelihood to be experimentally realized. The magnitude of the kinetic barriers will then determine which of *these* structures will actually be metastable.

The results for SnO$_2$ provide further support for the main arguments of this Letter. The two most frequent structures
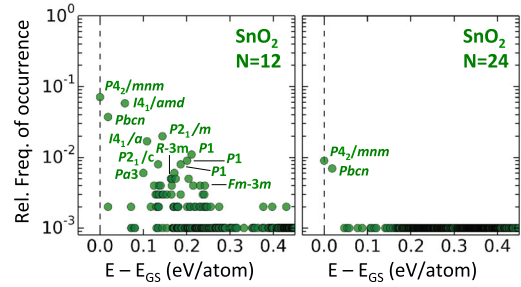
FIG. 4.   Results of the fixed size RSL sampling performed for SnO$_2$ for cells with 12 atoms (left panel, $N = 12$) and 24 atoms (right panel, $N = 24$). It is shown that the only two structures that remain as high occurrence structures for $N = 24$ are the two experimentally realized polymorphs, rutile ($P4_2/mnm$) and α-PbO$_2$ type ($Pbcn$).

in the RSL sampling are the ground state rutile $P4_2/mnm$ and the anatase $I4_1/amd$ structure. As indicated in Fig. 3, cubic Fm-$3m$ structure is dynamically unstable, and the fourth most frequent structure R-$3m$ is ~200 meV/atom above rutile. The metastable $Pbcn$ structure (α-PbO$_2$ type), that is observed in high pressure experiments, is the most frequent among the structures that have their energy close to, and volumes smaller than, the rutile phase. This explains why $Pbcn$ SnO$_2$ is typically observed upon releasing the pressure. Interestingly, the anatase SnO$_2$ predicted to be among the most probable structures has so far not been realized experimentally. It has a volume significantly larger than the rutile and, contrary to TiO$_2$ which has the rutile and anatase polymorphs nearly degenerate, has an energy by 58 meV/atom above rutile SnO$_2$. An important fact that emerges from the size analysis (Table III, Supplemental Material [33]) is that both anatase and R-$3m$ SnO$_2$ structures appear in the RSL sampling only for cell sizes with 12 or fewer atoms (also true for Fm-$3m$). Therefore, these two structures might potentially represent the already discussed situation where a local minimum appears large only in small dimensions. To test whether this is true the fixed size RSL sampling has been performed for SnO$_2$ for cells with 12 and 24 atoms. A total of 1000 RSL structures are generated for each size. The results are shown in Fig. 4. It is evident that for 12 atom cells (left panel, $N = 12$) the top occurring structures are rutile ($P4_2/mnm$), α-PbO$_2$ type ($Pbcn$), and anatase ($I4_1/amd$). Many other structures also appear to have relatively high occurrence. However, for $N = 24$, only the two experimentally realized structures known to exist at ambient conditions, i.e., the rutile and α-PbO$_2$ type, remain the high-frequency structures. This indicates the reasons behind the absence of anatase SnO$_2$ [40].

In conclusion, this Letter demonstrates that the random superlattice (RSL) structure sampling followed by the DFT relaxations can be used to screen different polymorphs of ionic systems as well as to assess the likelihood for their experimental realization. It is shown that the key quantity in

assessing the likelihood for experimental realization is the resulting frequency of occurrence, which is used as an estimate (indirect) of the volume of configuration space occupied by a given structure (its funnel of attraction). Application of the RSL sampling on MgO, ZnO, and SnO_2 reveals that the experimentally observed polymorphs are exclusively the ones that have the highest frequency (probability) of occurrence, consistently as the cell size used in sampling increases, explaining the physical reasons behind the experimental observations.

---

[*]vstevano@mines.edu

[1] L. J. Thernard and J. B. Biot, Mem. Phys. II. Soc. d'Arcueil **2**, 176 (1809).

[2] A. R. Verma and P. Krishna, *Polymorphism and Polytypism in Crystals* (John Wiley & Sons, Inc., New York, 1966).

[3] http://materials.springer.com.

[4] T. Luttrell, S. Halpegamage, J. Tao, A. Kramer, E. Sutter, and M. Batzill, Sci. Rep. **4**, 4043 (2014).

[5] S. Botti, J. A. Flores-Livas, M. Amsler, S. Goedecker, and M. A. L. Marques, Phys. Rev. B **86**, 121204 (2012).

[6] L. L. Baranowski, L. Krishna, A. D. Martinez, T. Raharjo, V. Stevanovic, A. C. Tamboli, and E. S. Toberer, J. Mater. Chem. C **2**, 3231 (2014).

[7] F. H. Stillinger, Phys. Rev. E **59**, 48 (1999).

[8] S. M. Woodley and R. Catlow, Nat. Mater. **7**, 937 (2008).

[9] S. Evrenk, A. Guzik, and C. S. Adjiman, *Prediction and calculation of crystal structures: methods and applications* (Springer, Cham Switzerland, 2014).

[10] J. Pannetier, J. Bassas-Alsina, J. Rodriguez-Carvajal, and V. Caignaert, Nature (London) **346**, 343 (1990).

[11] J. C. Schön and M. Jansen, Angew. Chem., Int. Ed. Engl. **35**, 1286 (1996).

[12] S. M. Woodley, P. D. Battle, J. D. Gale, and C. Richard A. Catlow, Phys. Chem. Chem. Phys. **1**, 2535 (1999).

[13] A. R. Oganov and C. W. Glass, J. Chem. Phys. **124**, 244704 (2006).

[14] G. Trimarchi and A. Zunger, Phys. Rev. B **75**, 104113 (2007).

[15] B. Meredig and C. Wolverton, Nat. Mater. **12**, 123 (2013).

[16] A. Laio and M. Parrinello, Proc. Natl. Acad. Sci. U.S.A. **99**, 12562 (2002).

[17] A. Barducci, M. Bonomi, and M. Parrinello, Comput. Mol. Sci. **1**, 826 (2011).

[18] D. J. Wales and J. P. K. Doye, J. Chem. Phys. A **101**, 5111 (1997).

[19] S. Goedecker, J. Chem. Phys. **120**, 9911 (2004).

[20] C. J. Pickard and R. J. Needs, J. Phys. Condens. Matter **23**, 053201 (2011).

[21] C. C. Fischer, K. J. Tibbetts, D. Morgan, and G. Ceder, Nat. Mater. **5**, 641 (2006).

[22] X. Zhang, V. Stevanović, M. d'Avezac, S. Lany, and A. Zunger, Phys. Rev. B **86**, 014109 (2012).

[23] R. Gautier, X. Zhang, L. Hu, L. Yu, Y. Lin, T. O. L. Sunde, D. Chon, K. R. Poeppelmeier, and A. Zunger, Nat. Chem. **7**, 308 (2015).

[24] M. A. Zwijnenburg, F. Illas, and S. T. Bromley, Phys. Rev. Lett. **104**, 175503 (2010).

[25] M. A. Zwijnenburg and S. T. Bromley, Phys. Rev. B **83**, 024104 (2011).

[26] T. D. Huan, M. Amsler, M. A. L. Marques, S. Botti, A. Willand, and S. Goedecker, Phys. Rev. Lett. **110**, 135502 (2013).

[27] A. Belsky, M. Hellenbrandt, V. L. Karen, and P. Luksch, Acta Crystallogr. Sect. B **58**, 364 (2002).

[28] A. B. M. A. Ashrafi, A. Ueta, A. Avramescu, H. Kumano, I. Suemune, Y.-W. Ok, and T.-Y. Seong, Appl. Phys. Lett. **76**, 550 (2000).

[29] F. Decremps, J. Pellicer-Porres, F. Datchi, J. P. Itié, A. Polian, F. Baudelet, and J. Z. Jiang, Appl. Phys. Lett. **81**, 4820 (2002).

[30] S. R. Shieh, A. Kubo, T. S. Duffy, V. B. Prakapenka, and G. Shen, Phys. Rev. B **73**, 014105 (2006).

[31] L.-G. Liu, Science **199**, 422 (1978).

[32] S. De, B. Schaefer, A. Sadeghi, M. Sicher, D. G. Kanhere, and S. Goedecker, Phys. Rev. Lett. **112**, 083401 (2014).

[33] See Supplemental Material at http://link.aps.org/supplemental/10.1103/PhysRevLett.116.075503 for further details on the results of the RSL sampling of MgO, ZnO and SnO_2.

[34] V. Stevanović, S. Lany, X. Zhang, and A. Zunger, Phys. Rev. B **85**, 115104 (2012).

[35] J. P. Perdew, K. Burke, and M. Ernzerhof, Phys. Rev. Lett. **77**, 3865 (1996).

[36] P. E. Blöchl, Phys. Rev. B **50**, 17953 (1994).

[37] G. Kresse and J. Furthmüller, Comput. Mater. Sci. **6**, 15 (1996).

[38] W. Press, *Numerical Recipes: The Art of Scientific Computing* (Cambridge University Press, Cambridge, England, 2007).

[39] https://github.com/pylada/pylada-light.

[40] The RSL sampling of TiO_2 polymorphs (results not included in this Letter) shows that the anatase TiO_2 is the high frequency structure for large cell sizes too, which explains why is this phase observed in TiO_2 and not in SnO_2.